scientific reports

Check for updates

OPEN

mPEG-PCL modified Caffeic acid eye drops for endotoxin-induced uveitis treatment

Yiping Wu[1], Lixu Wang[3], Chengda Hu[2] & Ruikang Tian[3]✉

The modulation of inflammatory mediators has emerged as a critical therapeutic strategy in uveitis management. Current nonsteroidal anti-inflammatory therapies face limitations due to systemic side effects. Caffeic acid (CA), a natural polyphenol with anti-inflammatory properties, holds therapeutic potential but suffers from poor solubility and ocular irritation. This study aimed to develop mPEG-PCL-modified CA-loaded nanoparticles (NanoCA) as a non-invasive eye drop formulation to enhance CA's solubility, bioavailability, and efficacy in treating endotoxin-induced uveitis (EIU). NanoCA was synthesized via the thin-film hydration method, characterized for size, zeta potential, drug loading, and release profile. Cytotoxicity was assessed in human corneal epithelial and RAW264.7 cells. Ocular tolerance was tested via slit-lamp and histopathological examinations. In vivo efficacy was evaluated in an EIU rat model using clinical scoring, histopathology, and immunofluorescence. NanoCA formed uniform nanospheres (42.40 ± 0.22 nm, -0.97 mV) with high encapsulation efficiency (99.17%). It exhibited sustained release over 12 h and reduced cytotoxicity compared to free CA. In EIU rats, NanoCA significantly suppressed inflammation, downregulated CD68 expression, and preserved aqueous barrier integrity. Histopathology confirmed minimal inflammatory infiltrates in NanoCA-treated eyes. The formulation demonstrated excellent ocular biocompatibility without corneal damage. NanoCA eye drops offer a safe, non-invasive therapeutic strategy for EIU, combining enhanced anti-inflammatory efficacy with high ocular tolerance. This nanoformulation presents a promising alternative to conventional CA delivery methods.

Keywords Anti-inflammatory, Endotoxin-induced uveitis, Caffeic acid, Eye drops, Nanoparticle

Uveitis is a severe ophthalmic disease that often leads to visual impairment and blindness[1,2]. It is an inflammatory disease of the iris, ciliary body, retina, and/or choroid. A significant increase in intraocular inflammation is its hallmark feature[3–6]. Nonsteroidal anti-inflammatory drugs can reduce the levels of ocular inflammatory factors, effectively suppressing ocular inflammation, and are the mainstay of current clinical treatment for uveitis (non-infectious)[7,8]. However, due to severe local side effects (i.e. cataracts, glaucoma) and systemic side effects, the long-term effectiveness of medication is very limited[9–11]. A low toxicity and effective anti-inflammatory drug is urgently needed.

With the development of pharmacy, more and more natural anti-inflammatory drugs have been widely discovered and studied. Caffeic acid (CA) is a member of natural polyphenolic compounds, exhibiting antioxidant, anti-inflammatory, and immunomodulatory properties. It can effectively inhibit the levels of inflammatory cytokines, and has shown promising effects in treating inflammatory corneal diseases and skin conditions[12–15]. It has been reported that CA derivatives administered through intraperitoneal injection in rat models of endotoxin-induced uveitis (EIU) effectively control inflammation[16,17]. Nevertheless, the limited water solubility of CA hampers its anti-inflammatory effects[18–22], and the use of insoluble particles on the ocular surface may cause discomfort and irritation[23]. Enhancing the solubility of CA may facilitate its anti-inflammatory function and improve its biocompatibility[18–22]. To achieve this goal, a new drug delivery system is required.

In the past few decades, considerable attention has been garnered for biodegradable polymeric micelles as a novel drug delivery system due to their high drug loading capacity, small particle size (less than 100 nm), and controllable drug release characteristics[24–26]. Monomethoxy poly(ethylene glycol)-poly (e-caprolactone) (mPEG-PCL) is a diblock copolymer that has been widely studied due to its stability and ease of surface modification.

[1]Eye Hospital of Shandong First Medical University, Jinan, Shandong, China. [2]The Second Affiliated Hospital and Yuying Children'S Hospital of Wenzhou Medical University, Wenzhou, Zhejiang, China. [3]State Key Laboratory of Ophthalmology, Optometry and Vision Science, Eye Hospital, Wenzhou Medical University, Wenzhou, Zhejiang, People's Republic of China325000. ✉email: 17861203656@163.com

It contains two segments: a lipophilic segment and a hydrophilic segment, which can form a lipophilic core and a hydrophilic shell in water. It has been proven that it can self assemble into micelles for the delivery of hydrophobic drugs[27–30]. In the present study, we hypothesized that mPEG-PCL micelles are a promising nanocarrier for CA. mPEG-PCL micelles can significantly enhance the water solubility and biocompatibility of CA, improving its bioavailability. And endow CA with better anti-inflammatory effects. As a proof of concept, we will further compare the in vivo therapeutic efficacy of mPEG-PCL micelles containing CA with that of CA suspension in a rat model.

Materials and method

Materials

Methoxy polyethylene glycol (mPEG) of varying molecular weights, poly εcaprolactone (PCL) and Sn (Oct)^2 were procured from Sigma-Aldrich (St. Louis, USA). Caffeic acid (CA) was purchased from Aladdin (Shanghai, China). Both the human corneal epithelial cells (HCECs) and RAW264.7 cells used in this study were obtained from ATCC (American Type Culture Collection, Manassas, Maryland, USA) and cultured under standard conditions as per the manufacturer's instructions. It is confirmed that all experiments were performed in accordance with relevant named guidelines and regulations. The protocols for using animals in this study were approved by the Animal Care and Ethics Committee at Wenzhou Medical University (Wenzhou, China). All experiments were conducted in compliance with the ARRIVE guidelines (https://arriveguidelines.org) and adhered to institutional and national regulations for the care and use of laboratory animals.

Synthesis and characterization of MPEG-PCL

The mPEG-PCL co-polymer was synthesized using the method reported before[28]. In short, mPEG, ε-CL and a small amount of Sn (Oct)^2 were poured into a three-necked flask, heated the oil bath to 160 ℃, and reacted under nitrogen atmosphere for 8 h. After the reaction was completed, the contents of the flask were dissolved in dichloromethane, and the resulting mixture was poured into cold petroleum ether with constant mechanical stirring to obtain the crude mPEG-PCL co-polymer, which was dialyzed in distilled water for 3 days to obtain the final mPEG-PCL co-polymer.

Preparation of CA micelles

CA micelles are prepared using the schemes outlined in previously published work[27,31]. In short, 10 mg of free CA and different amounts of mPEG-PCL copolymer were poured into a round-bottom flask, dissolved in a certain volume of acetone, and evaporated the contents of the flask to dryness with a rotary evaporator while heating in a water bath at 60 ℃, so that a film formed on the inner surface of the round-bottom flask. Subsequently, 10 mL of double distilled water was added to the round-bottom flask and the mixture was sonicated at 60 ℃ for 30 min to form NanoCA. Blank mPEG-PCL micelles without any drugs were synthesized by the same method. All micelles were filtered using 0.22-μm microporous filter and then freeze-dried into powder for further analysis.

Characterization of NanoCA

Transmission electron microscope observation (TEM)

The morphology of NanoCA was determined by transmission electron microscopy (Talos F200S, Thermo Fisher, USA). Samples (5 μL) were pipetted onto a copper grid and negatively stained with 0.5% (wt) phosphotungstic acid solution followed by drying in an oven overnight before observation.

Size measurement and zeta potential

The size distribution and zeta potential of mPEG-PCL micelles and various drug load ratios of NanoCA were analyzed using a Zetasizer Nano ZS-90 (Malvern Instruments, Malvern, UK). The samples were properly diluted with double distilled water, then filtered using a 0.22-μm microporous filter for measurement at 25 °C. Each measurement was repeated at least three times.

Drug Loading capacity (LC) and Encapsulation Efficiency (EE)

The determination of the Drug Loading capacity (LC) and Encapsulation Efficiency (EE) was carried out using high-performance liquid chromatography (Agilent 1200, Agilent Technologies, USA) at a wavelength of 323 nm. NanoCA was diluted with methanol to an appropriate multiple and filtered using a 0.22-μm microporous filter for further measurement. The mobile phase consisted of (A) methanol and (B) 0.5% glacial acetic acid (35:65 V/V). Separation was performed on a reverse-phase C18 column (4.6×150 mm, 5 μm). The column temperature was set to 25°C[32].

In vitro release study

The in vitro release behavior of NanoCA was performed by HPLC through dialysis method. In detail, 1 mL of 1 mg/ml NanoCA was placed in three dialysis bags (MW 8000–14,000 Da) respectively, and the bags were immersed in glass bottles, and 10 ml release medium (PBS, 0.1 mM with 0.5% Tween-80) was added to each dialysis bag. The entire system was placed in a 37 °C shaker incubator with 120 rpm continuous stirring. 1 mL of release medium was taken from each dialysis bag at predetermined time intervals and 1 mL of fresh release medium was replenished. The withdrawn medium was filtered through 0.22-μm microporous filter for HPLC analysis.

In vitro cytotoxicity assay

HCECs and RAW264.7 cells were used to assess the in vitro cytotoxicity of CA and NanoCA using the MTT assay. HCECs were cultured in DMEM/F12 medium supplemented with 10% Fetal Bovine Serum (FBS) and

1% penicillin–streptomycin (Pen-Strep). RAW264.7 cells were cultured in Dulbecco's Modified Eagle Medium (DMEM) supplemented with 10% FBS and 1% Pen-Strep. Briefly, HCECs or RAW264.7 cells were seeded into a 96-well plate at a density of 1×10^4 cells/well and incubated in a CO_2 incubator at 37 °C overnight. Subsequently, a series of free CA and NanoCA at different concentrations (25–800 μM) were added to each well for co-incubation. After 24 h of incubation, 20 μL of MTT solution was added to each well, and the mixture was incubated for another 2 h, followed by the addition of DMSO to dissolve the formazan. Finally, the absorbance of each well was measured at 490 nm using a microplate reader (Molecular Devices, SpectraMax190, USA). The untreated cells were used as controls. Cell viability was calculated using the following formula: cell viability (%) = absorbance of the tested sample/absorbance of the control sample × 100.

Ocular irritation test

Four male Sprague Dawley rats (weighting: 200–250 g) were used for the ocular irritation test. Briefly, 30 μL of NanoCA (5 mM) or PBS (pH 7.4) were instilled (6 times in 24 h) into the conjunctival sac of eyes, and the clinical signs of each eye were evaluated and graded by an experienced ophthalmologist at 24 h post-instillation using a slit lamp. The sodium fluorescein staining assay was conducted 24 h post-instillation to evaluate the integrity of the corneal epithelium. After 24 h, the rats were sacrificed, and their eyeballs were harvested for histopathological observation using H&E staining.

In vivo pharmacodynamic evaluation

EIU induction and treatment

The EIU model was induced following the protocol described in previous reports[16,17]. In brief, 6–8 weeks old male Sprague Dawley rats (weighting: 200–250 g) were housed at the Laboratory Animal Service Center of the Wenzhou Medical University and purchased from Beijing Vital River Laboratory Animal Technology Co., Ltd. The rats were maintained at 25℃ with 12 h light and 12 h dark cycles, with free access to food and water. All the rats were anesthetized with inhaled isoflurane for the surgery and 2.0% pentobarbital sodium for sacrifice. Animals were randomly divided into five groups: a normal group (WT group); EIU group (LPS group); Blank MPEG-PCL micelles treatment group (LPS + Blank micelle group); free CA treatment group (LPS + free CA group); and NanoCA treatment group (LPS + NanoCA group). A total number of 20 SD rats were used in this study (n = 4 per group). Lipopolysaccharide (LPS) was dissolved in phosphate buffer saline (PBS) and EIU was induced by the injection of 0.1 mL of 1 mg/kg LPS solution into two footpads. On the first day, the WT group and the LPS group both received eye drops six times a day of 30 μL PBS. The LPS + Blank micelle group, LPS + free CA group and LPS + NanoCA group received eye drops six times a day of 30 μL Blank mPEG-PCL micelle, 30 μL free CA (5 mM) and 30 μL NanoCA (5 mM) respectively. All the animal experiments were conducted under the supervision and approval of the Wenzhou Medical University Institutional Animal Care and Use Committee.

Clinical and histological assessment of EIU

Clinical scores of each group were evaluated at 24 h after induction of the EIU with a slit lamp microscope (SLM-8E, Chongqing Kang Huarui Ming Technology co., LTD). The standard of the clinical score was as follows: 0 = no disease; 1 = mild iris hyperemia, miotic pupil, small exudate in anterior chamber and present hypopyon; 2 = moderate iris hyperemia and large exudate in anterior chamber; 3 = severe iris hyperemia. Inflammatory signs and scores were recorded, and photographs were taken.

At the end of the experiment, the eyes of each group were freshly harvested, fixed, embedded into wax, and sliced into 5-μm sections, and stained with hematoxylin and eosin for histological evaluation. The histological assessment for sections of each group was based on the number of inflammatory cell as follows: 0 = healthy retinal structure, no inflammatory cells/field; 1 = mild inflammatory cells (1 to 10 cells)/field; 2 = moderate inflammatory cells (11 to 30 cells)/field; 3 = excessive inflammatory cells (30 to 100 cells)/field; 4 = excessive inflammatory cell (101 to 300 cells)/field.

Immunofluorescence assay

After all eyeballs were collected, fixed in 4% paraformaldehyde and embedded in OCT compound, the retinas were sliced into 10-μm thick sections. First, the sections were blocked with blocking solution (Beyotime Biotechnology, China), incubated with the following primary antibodies overnight: CD68 (Bio-Rad, MCA341GA), and then fluorescence-conjugated secondary antibodies (1:500, Invitrogen) were applied to detect the positive signal. Finally, DAPI was used to stain the cell nuclei. The number of positive cells and mean fluorescence values were quantified by Image J software.

Statistical analysis

The results of all experiments are expressed as the mean ± SD. In vitro cytotoxicity, in vitro anti-inflammatory efficacy and in vitro animal model assay data were analyzed using one-way analysis of variance (ANOVA) with Tukey's multiple comparisons test using GraphPad Prism (version 9.4.1). Statistical significance was set at $p < 0.05$.

Results and discussion

Fabrication and characterization of NanoCA

In our study, we established three groups with drug/polymer ratios of 1/2, 1/5, and 1/10 for the determination of loading content (LC) and encapsulation efficiency (EE). As illustrated in Table 1, the NanoCA group with a 1/5 ratio exhibited optimal characteristics, with an LC of 16.55 ± 1.20% and an EE of 99.17 ± 0.65%. Consequently, this ratio was selected for further experimentation. Figure 1B demonstrates that under laser illumination, a 5 mM solution of free CA remained clear, while a 5 mM NanoCA solution exhibited the Tyndall effect, indicating

Drug/polymer ratio	PDI	Mean particle size (nm)	Zeta potential (mV)	EE(%)	LC(%)
1/2	0.09 ± 0.01	29.76 ± 0.11	−0.88 ± 0.40	45.20 ± 3.94	18.43 ± 1.39
1/5	0.14 ± 0.01	42.40 ± 0.22	−0.97 ± 0.22	99.17 ± 0.65	16.55 ± 1.20
1/10	0.21 ± 0.01	44.11 ± 0.14	−2.49 ± 0.06	78.44 ± 1.69	7.27 ± 0.73

Table 1. EE (%) and LC (%) of the NanoCA solution with various ratios.

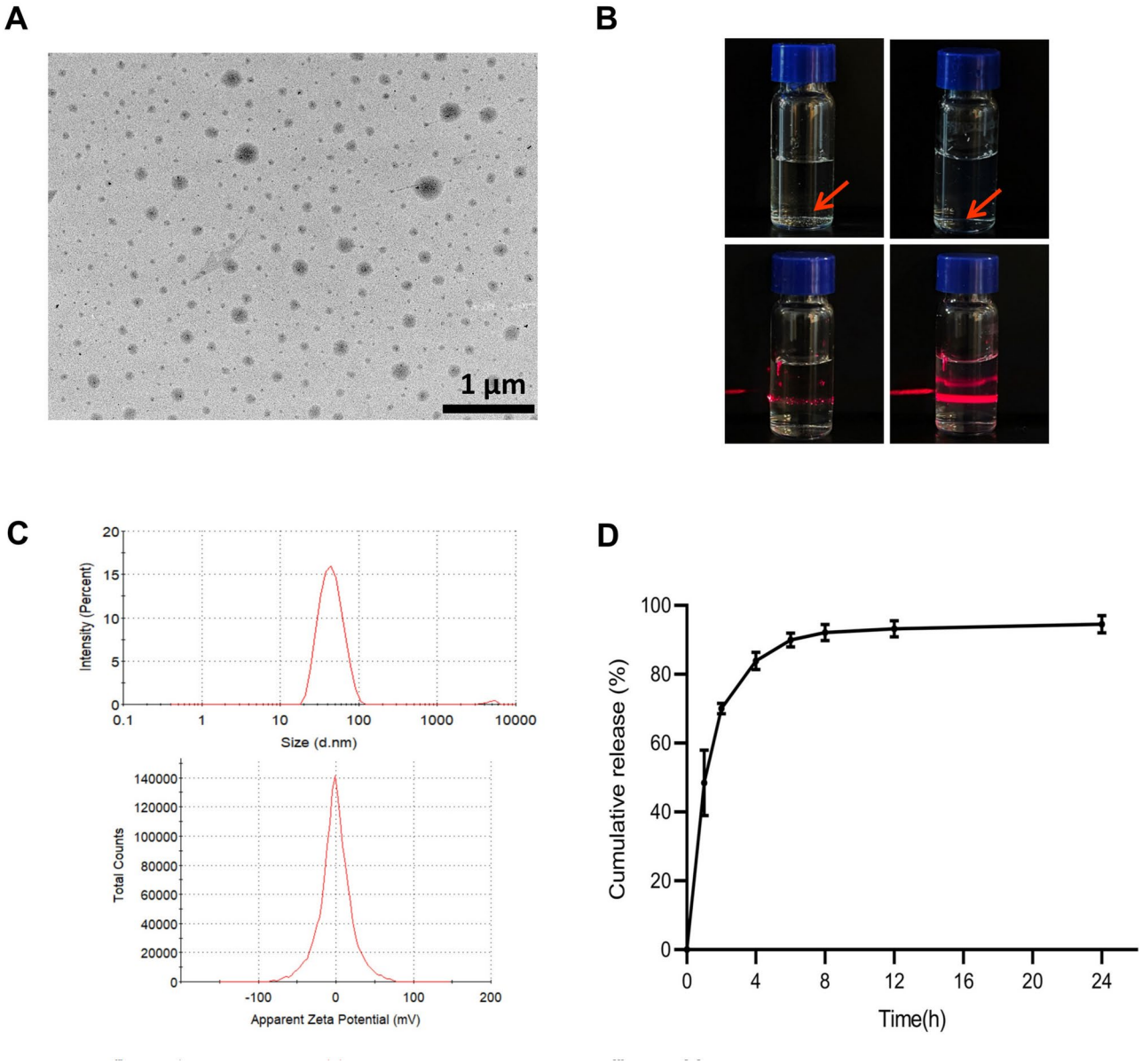

Fig. 1. (**A**) TEM image of the NanoCA solution. (**B**) Visual comparison of freeCA (left) and NanoCA (right) solutions at 5 mM. Red arrow: dissolved state; laser light: Tyndall effect. (**C**) Size distribution and zeta potential of NanoCA solution. (**D**) In vitro cumulative release (%) profile of NanoCA solution.

a colloidal state. Transmission electron microscopy (TEM) results, shown in Figs. 1A and 1 C, revealed the formation of uniformly distributed nanospheres with an average diameter of 42.40 ± 0.22 nm. The Zeta potential measurement of the NanoCA particles was −0.97 ± 0.22 mV (Fig. 1C), and complete drug release was achieved within 12 h (Fig. 1D).

In vitro cytotoxicity assay

An in vitro cytotoxicity assessment was conducted using the MTT assay to evaluate the potential cytotoxic effects of free CA and NanoCA on HCECs and RAW264.7 cells. As shown in Figs. 2A and 2B, CA demonstrated dose-dependent cytotoxicity in both HCECs and RAW264.7 cells, with cell viability decreasing to approximately 50% at a concentration of 800 μM. This is consistent with previous reports that natural CA causes varying degrees of decreased viability in HCEC and RAW264.7 cell lines[20,33,34]. In contrast, NanoCA at concentrations up to 400 μM did not exhibit significant cytotoxicity in either cell line. These findings indicate that the cytotoxicity of native CA was significantly mitigated through mPEG-PCL nanoencapsulation.

Efficacy of the in vivo rat EIU model

As illustrated in Fig. 3A, we established the classical EIU model by administering LPS into the footpads of rats, followed by immediate drug treatment at 4-h intervals for a total of 6 doses. The eyes were examined the following day using a slit lamp. Figures 3B and 3C show that mPEG-PCL alone had no therapeutic effect on EIU, similar to PBS. Local administration of 5 mM free CA in rat eyes produced a slight therapeutic effect, with some residual pus formation. In contrast, our newly synthesized NanoCA exhibited a potent therapeutic effect against EIU. Rats treated with NanoCA displayed minimal pus in the anterior chambers and pupil sizes comparable to those of the Normal group. These results indicate that NanoCA eye drops significantly enhance the anti-inflammatory effects in the treatment of EIU.

Analysis of immunofluorescence and pathological section results

Rat eyeballs treated with PBS, mPEG-PCL, 5 mM CA, and 5 mM NanoCA were removed for tissue staining with H&E and immunofluorescence. As depicted in Fig. 4, the mPEG-PCL group exhibited high expression of the classical inflammation signal CD-68, similar to PBS. While the CA group showed reduced CD-68 expression, it was still present. Only the NanoCA group, akin to the Normal group, exhibited no CD-68 inflammation signal. Furthermore, H&E staining revealed that only the NanoCA group maintained the integrity of the rat aqueous barrier. These findings further support the notion that our newly synthesized NanoCA enhances the anti-inflammatory effects of CA, thereby inhibiting the progression of EIU and demonstrating excellent therapeutic outcomes.

Ocular irritation test

As shown in Fig. 5, after 24 h of topical instillation of NanoCA and PBS on the rat corneas (every 4 h), slit lamp and H&E slice observations were conducted. As illustrated, NanoCA did not induce irritation or corneal defects on the rat corneas under slit lamp examination. H&E slice observations revealed no structural damage to the cornea caused by NanoCA. These findings highlight the excellent ocular tolerance and biocompatibility of our newly synthesized NanoCA, making it a promising eye drop for EIU treatment.

Conclusion

In conclusion, we successfully developed a novel nano-formulated eye drop by encapsulating CA into mPEG-PCL micelles, which self-assembled into uniform nanoparticles with an average diameter of 42.40 ± 0.22 nm, a zeta potential of −0.97 ± 0.22 mV, and a high encapsulation efficiency of 99.17 ± 0.65%. Compared to free CA, NanoCA demonstrated significantly enhanced therapeutic efficacy in a rat model of EIU. Specifically, NanoCA-treated rats exhibited markedly reduced clinical scores, minimal anterior chamber exudate, and near-normal pupil sizes, whereas free CA showed only partial improvement. Histological and immunofluorescence analyses further confirmed that NanoCA effectively suppressed CD68 expression and preserved aqueous barrier integrity, outperforming both free CA and blank micelles.

The superior performance of NanoCA stems from its improved water solubility and sustained drug release profile. Importantly, NanoCA mitigated the cytotoxicity of free CA, maintaining > 80% cell viability in HCECs and RAW264.7 macrophages at therapeutic concentrations (400 μM), compared to ~ 50% viability with free CA

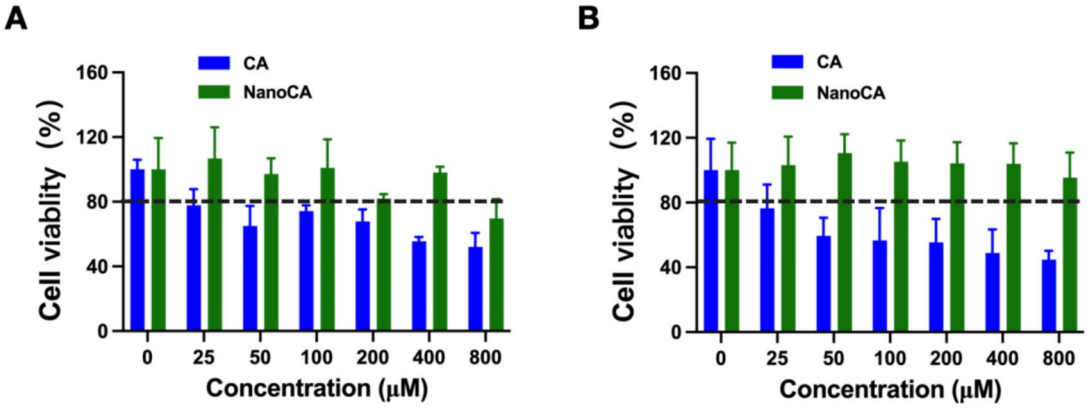

Fig. 2. In vitro cytotoxicity of free CA and NanoCA against (**A**) HCECs and (**B**) RAW264.7 cells.

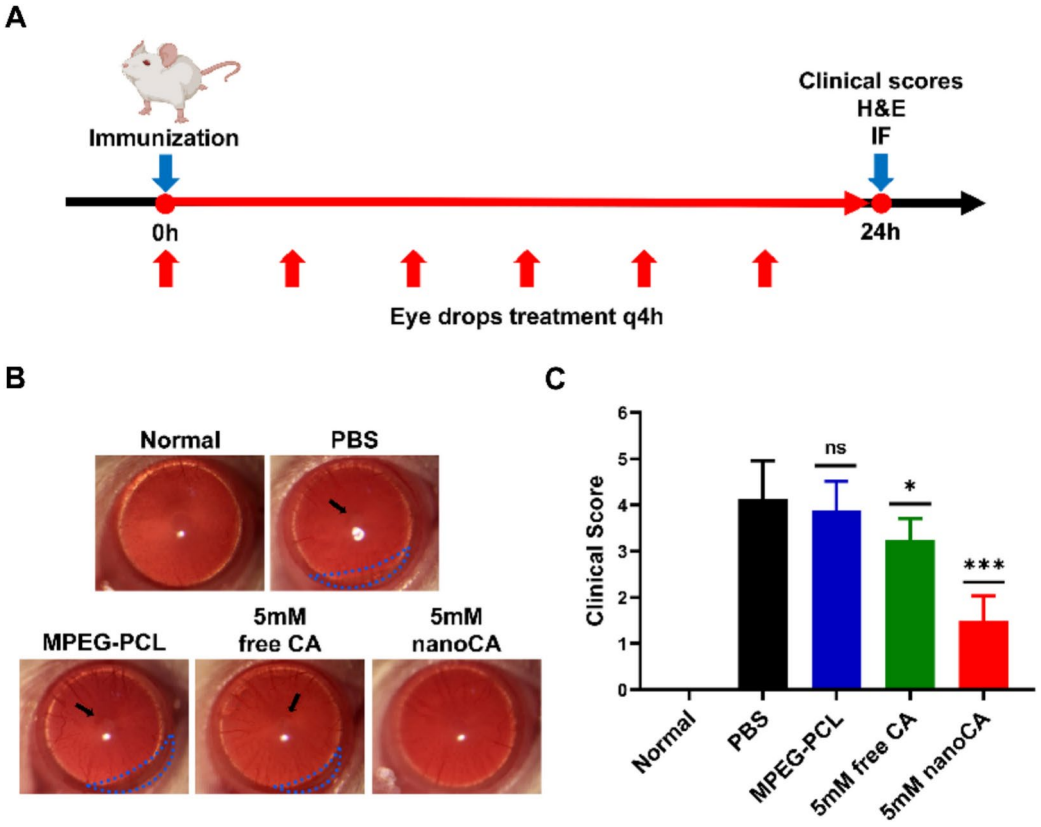

Fig. 3. (**A**) Schematic diagram of the treatment protocol for the rat EIU model. (**B**) Observation with slit lamp 24 h post-treatment. Black arrow: pupil adhesion, blue dotted circle: hypopyon. (**C**) Clinical scores of rats with EIU after treatment with PBS, MPEG-PCL, free CA (5 mM), and NanoCA (5 mM). n = 4 per group; *$p < 0.05$, ***$p < 0.001$ vs. the PBS group; ns, no significance.

at 800 μM. Furthermore, ocular irritation tests confirmed NanoCA's excellent biocompatibility, with no corneal damage or structural disruption observed.

These findings highlight NanoCA as a promising non-invasive therapeutic strategy for non-infectious uveitis, addressing the limitations of conventional CA formulations. Future studies will focus on optimizing dosage regimens and exploring long-term safety to advance clinical translation.

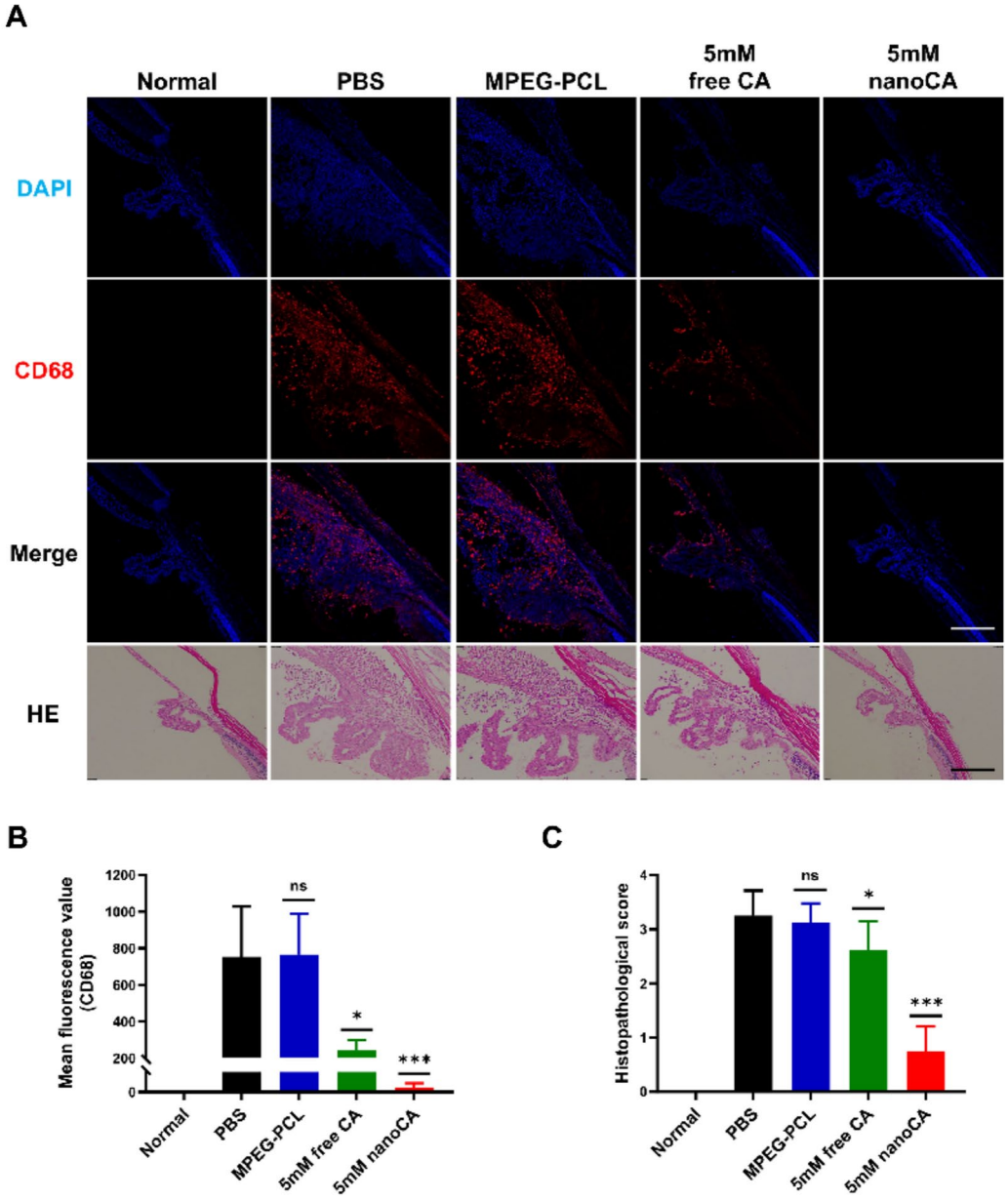

Fig. 4. Histological and immunohistochemical analysis. (**A**) Representative immunofluorescence staining and H&E staining showing rats with EIU after treatment of PBS, mPEG-PCL, free CA (5 mM) and NanoCA (5 mM). (**B**) Quantitative analysis of CD68 mean fluorescence intensity. (**C**) Histopathological EIU scores at 24 h post-treatment. n = 4 per group; *$p < 0.05$, *** $p < 0.001$ vs. the PBS group; ns, no significance.

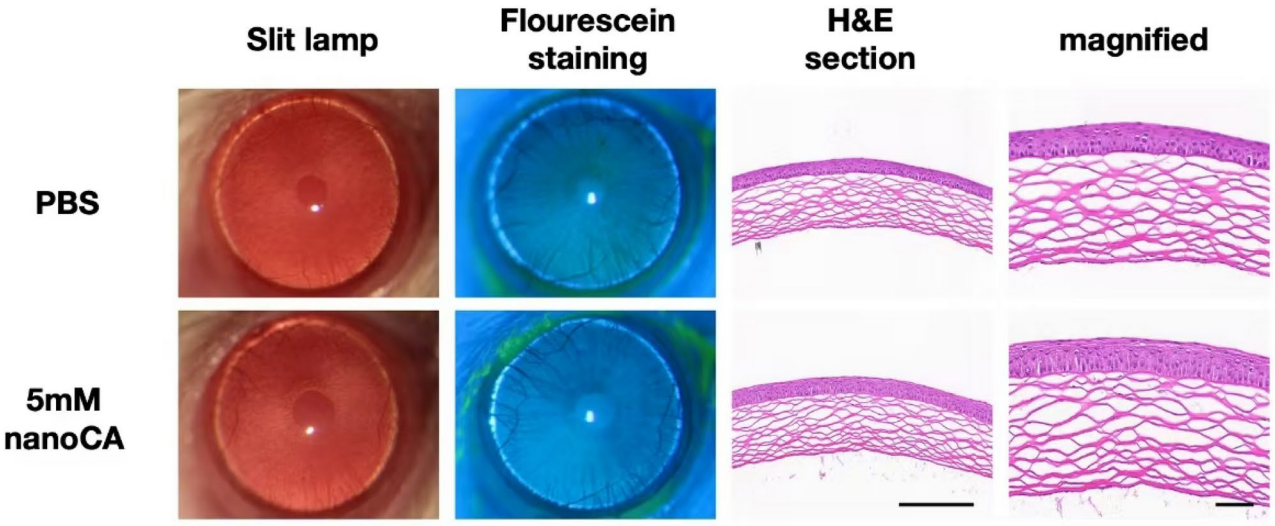

Fig. 5. Representative slit lamp images and H&E sections of PBS and NanoCA treated eyes at 24 h postmedication.

Data availability

The data that support the findings of this study are available on request from the corresponding author.

Received: 30 December 2024; Accepted: 12 March 2025
Published online: 15 March 2025

References

1. Forrester, J. V., Kuffova, L. & Dick, A. D. Autoimmunity, Autoinflammation, and Infection in Uveitis. *Am. J. Ophthalmol.* **189**, 77–85 (2018).
2. Foster, C. S. et al. The ocular immunology and uveitis foundation preferred practice patterns of uveitis management. *Surv. Ophthalmol.* **61**(1), 1–17 (2016).
3. Xu, J. et al. Aqueous cytokine levels in four common uveitis entities. *Int. Immunopharmacol.* **78**, 106021 (2020).
4. Bonacini, M. et al. Cytokine profiling in aqueous humor samples from patients with non-infectious uveitis associated with systemic inflammatory diseases. *Front. Immunol.* **10**(11), 358 (2020).
5. Ahn, J. K., Yu, H. G., Chung, H. & Park, Y. G. Intraocular cytokine environment in active Behçet uveitis. *Am. J. Ophthalmol.* **142**(3), 429–434 (2006).
6. Takase, H. et al. Cytokine profile in aqueous humor and sera of patients with infectious or noninfectious uveitis. *Invest. Ophthalmol. Vis. Sci.* **47**(4), 1557–1561 (2006).
7. Imrie, F. R. & Dick, A. D. Nonsteroidal drugs for the treatment of noninfectious posterior and intermediate uveitis. *Curr. Opin. Ophthalmol.* **18**(3), 212–219 (2007).
8. Bucolo, C. et al. Effects of topical indomethacin, bromfenac and nepafenac on lipopolysaccharide-induced ocular inflammation. *J. Pharm. Pharmacol.* **66**(7), 954–960 (2014).
9. Kulkarni, P. Review: Uveitis and immunosuppressive drugs. *J. Ocul. Pharmacol. Ther.* **17**(2), 181–187 (2001).
10. Uchiyama, E., Papaliodis, G. N., Lobo, A. M. & Sobrin, L. Side-effects of anti-inflammatory therapy in uveitis. *Semin. Ophthalmol.* **29**(5–6), 456–467 (2014).
11. Lee, F. F. & Foster, C. S. Pharmacotherapy of uveitis. *Expert. Opin. Pharmacother.* **11**(7), 1135–1146 (2010).
12. Pavlíková, N. Caffeic acid and diseases-mechanisms of action. *Int. J. Mol. Sci.* **24**(1), 588 (2022).
13. Zhao, X., Liu, Z., Liu, H., Guo, J. & Long, S. Hybrid molecules based on caffeic acid as potential therapeutics: A focused review. *Eur. J. Med. Chem.* **5**(243), 114745 (2022).
14. Zielińska, D. et al. Caffeic acid modulates processes associated with intestinal inflammation. *Nutrients.* **13**(2), 554 (2021).
15. Touaibia, M., Jean-François, J. & Doiron, J. Caffeic acid, a versatile pharmacophore: An overview. *Mini. Rev. Med. Chem.* **11**(8), 695–713 (2011).
16. Yilmaz, A. et al. Effects of caffeic acid phenethyl ester on endotoxin-induced uveitis in rats. *Curr. Eye Res.* **30**(9), 755–762 (2005).
17. Jin, X. H. et al. Effects of blue honeysuckle (Lonicera caerulea L.) extract on lipopolysaccharide-induced inflammation in vitro and in vivo. *Exp. Eye Res.* **82**(5), 860–867 (2006).
18. Mude, H., Maroju, P. A., Balapure, A., Ganesan, R. & Ray, D. J. Water-soluble caffeic acid-dopamine acid-base complex exhibits enhanced bactericidal, antioxidant, and anticancer properties. *Food Chem.* **16**(374), 131830 (2022).
19. Kfoury, M., Geagea, C., Ruellan, S., Greige-Gerges, H. & Fourmentin, S. Effect of cyclodextrin and cosolvent on the solubility and antioxidant activity of caffeic acid. *Food Chem.* **25**(278), 163–169 (2019).
20. Li, Y. et al. Transglycosylation improved caffeic acid phenethyl ester anti-inflammatory activity and water solubility by leuconostoc mesenteroides dextransucrase. *J. Agric. Food Chem.* **67**(16), 4505–4512 (2019).
21. Meneses, C. C. F. et al. Caffeic acid-zinc basic salt/chitosan nanohybrid possesses controlled release properties and exhibits in vivo anti-inflammatory activities. *Molecules.* **28**(13), 4973 (2023).
22. Mude, H., Balapure, A., Thakur, A., Ganesan, R. & Ray, D. J. Enhanced antibacterial, antioxidant and anticancer activity of caffeic acid by simple acid-base complexation with spermine/spermidine. *Nat. Prod. Res.* **36**(24), 6453–6458 (2022).

23. Li, J. et al. Fabrication of a drug delivery system that enhances antifungal drug corneal penetration. *Drug. Deliv.* **25**(1), 938–949 (2018).
24. Kataoka, K., Harada, A. & Nagasaki, Y. Block copolymer micelles for drug delivery: Design, characterization and biological significance. *Adv. Drug. Deliv. Rev.* **47**(1), 113–131 (2001).
25. Ke, X. et al. Role of non-covalent and covalent interactions in cargo loading capacity and stability of polymeric micelles. *J. Control. Release* **10**(193), 9–26 (2014).
26. Binkhathlan, Z. et al. Role of polymeric micelles in ocular drug delivery: An overview of decades of research. *Mol. Pharm.* **20**(11), 5359–5382 (2023).
27. Song, Z. et al. Linear-dendrimer type methoxy-poly (ethylene glycol)-b-poly (ε-caprolactone) copolymer micelles for the delivery of curcumin. *Drug. Deliv.* **22**(1), 58–68 (2015).
28. Kheiri Manjili, H. et al. Pharmacokinetics and in vivo delivery of curcumin by copolymeric mPEG-PCL micelles. *Eur. J. Pharm. Biopharm.* **116**, 17–30 (2017).
29. Peng, W. et al. Oral delivery of capsaicin using MPEG-PCL nanoparticles. *Acta Pharmacol. Sin.* **36**(1), 139–148 (2015).
30. Kurd, M., Sadegh Malvajerd, S., Rezaee, S., Hamidi, M. & Derakhshandeh, K. Oral delivery of indinavir using mPEG-PCL nanoparticles: preparation, optimization, cellular uptake, transport and pharmacokinetic evaluation. *Artif. Cells Nanomed. Biotechnol.* **47**(1), 2123–2133 (2019).
31. Dash, T. K. & Konkimalla, V. B. Poly-ε-caprolactone based formulations for drug delivery and tissue engineering: A review. *J. Control. Release* **158**(1), 15–33 (2012).
32. Guan, Q. et al. Docetaxel-loaded self-assembly stearic acid-modified bletilla striata polysaccharide micelles and their anticancer effect: Preparation, characterization, cellular uptake and in vitro evaluation. *Molecules.* **21**(12), 1641 (2016).
33. Wu, Y. et al. Nano self-assemblies of caffeic acid-fibronectin mimic a peptide conjugate for the treatment of corneal epithelial injury. *Mol. Pharm.* **20**(11), 5937–5946 (2023).
34. Ren, Z. et al. Mitochondrial localization of antioxidant nanodrug suppresses ocular inflammation by alleviating oxidative stress on cells. *Chemistry* **31**(10), e202402441 (2025).

Author contributions

Design of the study: YW; conduct of the study and data collection: YW; analysis and interpretation and manuscript preparation and review: YW, LW, CH and RT. All authors read and approved the final version of the article.

Funding

This research did not receive any specific grant from funding agencies in the public, commercial, or not-for-profit sectors.

Declarations

Competing interests

The authors declare no competing interests.

Additional information

Correspondence and requests for materials should be addressed to R.T.

Reprints and permissions information is available at www.nature.com/reprints.

Publisher's note Springer Nature remains neutral with regard to jurisdictional claims in published maps and institutional affiliations.